

Formation of current-vortex filaments

Y. Yatsuyanagi and T. Ebisuzaki

Computational Science Division, RIKEN (The Institute of Physical and Chemical Research), Wako-shi, Saitama 351-0198, Japan

T. Hatori

Department of Information Science, Kanagawa University, Hiratsuka-shi, Kanagawa 259-1293, Japan

T. Kato

Department of Applied Physics, Waseda University, Shinjuku-ku, Tokyo 169-8555, Japan

(Received 24 July 2001; accepted 8 November 2001)

Time evolution of a system where electric current and vorticity coexist is demonstrated by two-dimensional magnetohydrodynamic simulations. Such a system has two characteristics. The first one is that once the electric current and the vorticity share the same position, they tend to move simultaneously, staying overlapped with each other. The second one is that the electric current and the vorticity evolve to create more overlapping regions where they coexist, even if their initial spatial distributions are not the same. During the evolution, the distributions of the electric current and the vorticity are fragmented, and the current-vortex filaments are formed. Once the current-vortex filaments are formed, they survive stably. This is due to the strong correlation between the electric current and the vorticity. © 2002 American Institute of Physics.

[DOI: 10.1063/1.1432317]

I. INTRODUCTION

Our final goal is to demonstrate a detailed mechanism of the solar flare. Many researchers now share a common concept that fast magnetic reconnection should be a main mechanism for the solar flare. However, the details still remain unclear. Thus considerable attention has been devoted to the theory of fast magnetic reconnection.¹⁻⁴ We proposed a chaotic reconnection model as a candidate for the fast magnetic reconnection model.⁵⁻⁸ An illustration of the chaotic reconnection model is shown in Fig. 1. In this model, we assume that the magnetic fields in the reconnection region should be in chaotic configuration, which yields the fast process. To demonstrate the mechanism of the chaotic reconnection, we analyzed the dynamics of the current-vortex filaments through both analytic and numerical methods.^{5,6} The current-vortex filament has the electric current and the vorticity along its axis. In the simulations concerning a collision between the two current-vortex filaments, it is found that they are tangled with each other with time. The configuration of the tangled filaments is found to be chaotic owing to the turbulent flow induced by themselves. Then, we concluded that a reconnection probability (rate) of the filaments is extremely enhanced by the chaotic configuration. This is a basic idea of the chaotic reconnection.

In the model mentioned above, we presumed that the electric current and the vorticity were confined in the same filament at the initial state. To give a well-grounded basis for this assumption, it has to be revealed how the electric current and the vorticity align and form the filaments. Thus, in this paper we investigate the time evolution of a system including the electric current and the vorticity through numerical simulations. Such a system involves the Kelvin-Helmholtz instability and/or the tearing instability.⁹ Demonstration of the

formation of the current-vortex filaments will provide a basis for the chaotic reconnection model in the previous work.

In this paper, we present results of two-dimensional magnetohydrodynamic (MHD) simulations that demonstrate the formation of the current-vortex filaments. A main parameter of the simulations is the initial distributions of the electric current and the vorticity. To analyze the alignment between the electric current and the vorticity quantitatively, we define two new factors. They are a total alignment factor and an antiparallel alignment factor. The alignment factors give a measure to determine how much the electric current and the vorticity occupy the same position on x - y plane.

When initial spatial distributions of the electric current and the vorticity are the same, the electric current and the vorticity tend to move simultaneously, staying overlapped with each other. This means a strong correlation between the electric current and the vorticity.

When the initial spatial distributions are not the same, the magnetic reconnection and/or the velocity field line reconnection occurs. Discontinuous initial current sheets make the magnetic reconnection dominant. Then, the distribution of the vorticity fragments. On the other hand, discontinuous initial vortex sheets make the velocity field line reconnection dominant. Then, the distribution of the electric current fragments. It is remarkable that in both cases, the time-evolved distributions of the electric current and the vorticity become quite similar. The resulting distributions indicate the formation of the current-vortex filaments. Once the current-vortex filaments are formed, they survive stably. This is due to the strong correlation between the electric current and the vorticity mentioned above.

From these results, we conclude the following two points. The first one is that once the electric current and the

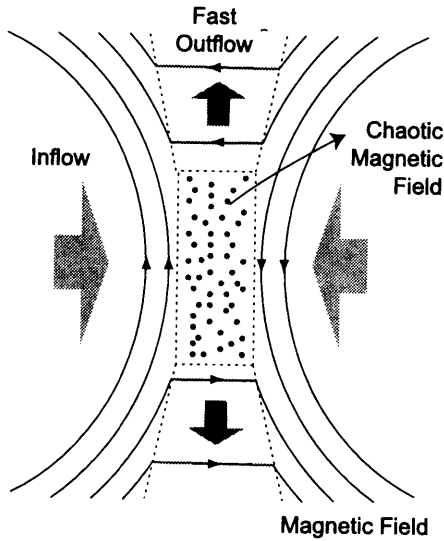


FIG. 1. Illustration of the chaotic reconnection model is shown.

vorticity share the same position, they tend to move simultaneously, staying overlapped with each other. The second one is that the electric current and the vorticity evolve to create more overlapping regions where they coexist, even if their initial spatial distributions are not the same. Then, the current-vortex filaments are formed because there are many regions where the electric current and the vorticity coexist.

The paper is organized as follows: In Sec. II, we present basic equations and a simulation model. In Sec. III, we show simulation results. We also introduce the alignment factors. In Sec. IV, we give conclusions.

II. BASIC EQUATIONS AND SIMULATION MODEL

We use the two-dimensional resistive MHD equations:

$$\frac{\partial \omega_z}{\partial t} = -(\mathbf{u} \cdot \nabla) \omega_z + (\mathbf{B} \cdot \nabla) j_z, \quad (1)$$

$$\frac{\partial A_z}{\partial t} = -(\mathbf{u} \cdot \nabla) A_z + \frac{\eta}{\mu_0} \nabla^2 A_z, \quad (2)$$

$$\nabla \cdot \mathbf{u} = 0, \quad (3)$$

$$\mathbf{E} + \mathbf{u} \times \mathbf{B} = \eta \mathbf{j}, \quad (4)$$

$$\mathbf{B} = -\hat{\mathbf{z}} \times \nabla A_z, \quad (5)$$

$$\omega_z = (\nabla \times \mathbf{u}) \cdot \hat{\mathbf{z}}, \quad (6)$$

$$j_z = (\nabla \times \mathbf{B}) \cdot \hat{\mathbf{z}}, \quad (7)$$

where \mathbf{B} and \mathbf{u} are the magnetic field and the velocity on the x - y plane, A_z , j_z , and ω_z are the z components of the magnetic vector potential, the electric current density and the vorticity, respectively. The unit vector in z direction is denoted by $\hat{\mathbf{z}}$. The classical electric resistivity is denoted by η .

Initial configurations of the simulations are shown in Fig. 2. The velocity is normalized by the Alfvén velocity. All the length parameters are normalized by the initial sheet widths of the electric current and the vorticity L_0 , which are the same in all the initial configurations. The size of the

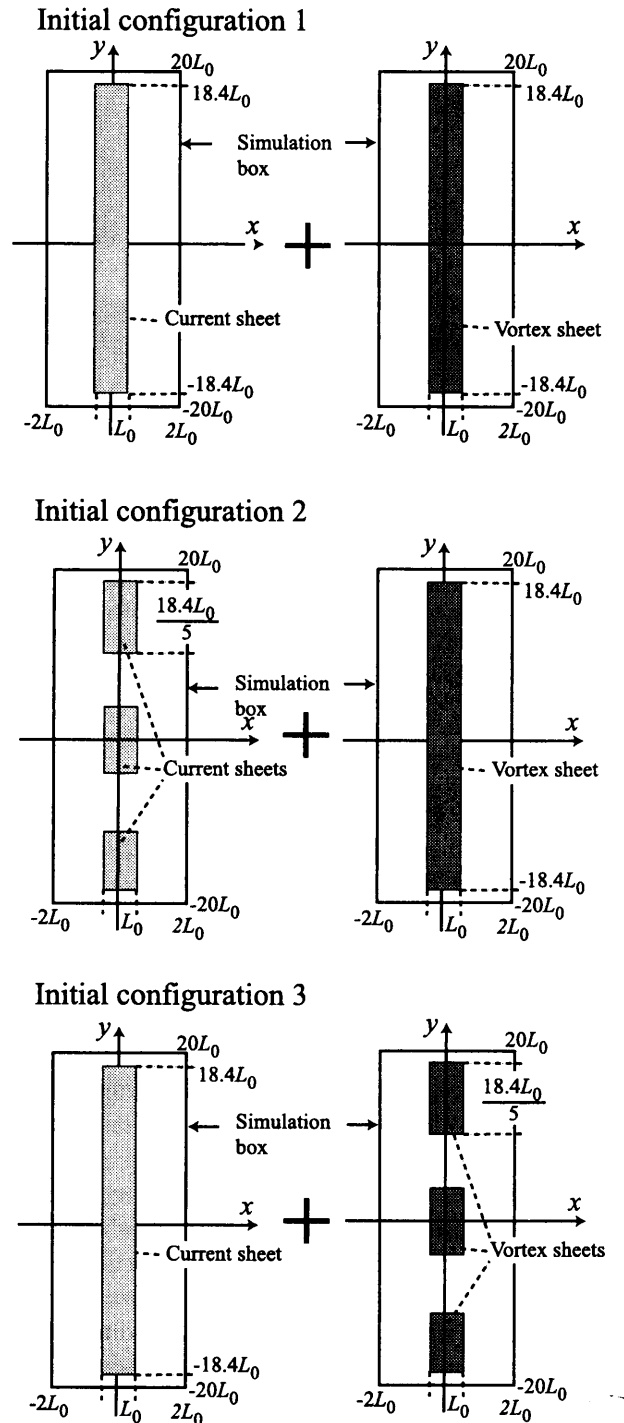


FIG. 2. The initial conditions of simulations are shown.

simulation box is $4L_0$ in the x direction and $40L_0$ in the y direction. Both the current and the vortex sheets have finite length in the y direction.

We use three different initial configurations, 1–3. For initial configuration 1, the lengths of the current and the vortex sheets are $36.8L_0$ each. Both the sheets perfectly overlap with each other and form the current-vortex sheet. For initial configuration 2, there are three current sheets and one vortex sheet. Namely, there are three current-vortex sheets, and two vortex sheets are located between the current-vortex sheets. Each length of the current sheet in the y direction is reduced to $1/5$ ($7.4L_0$) compared with that for initial configuration 1, while the length of the vortex sheet is unchanged. In this case, the magnetic reconnection may be the dominant pro-

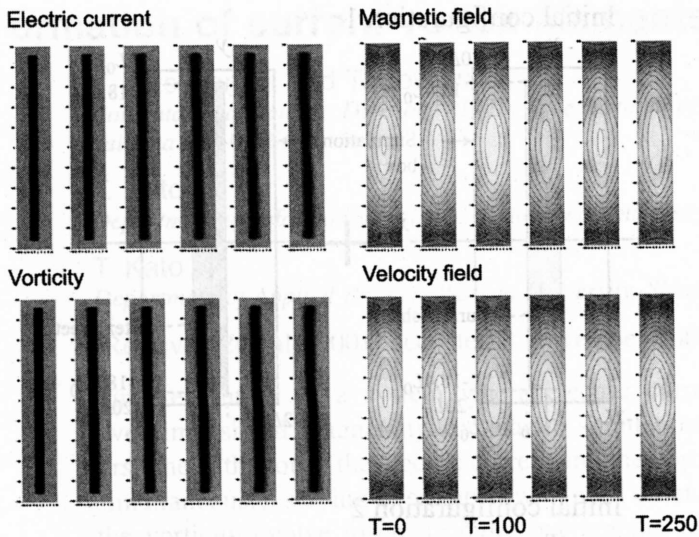


FIG. 3. Time evolutions of the distributions of the electric current density, the vorticity, the magnetic vector potential and the stream function for type (a) are shown. The figures are the contour plots of them on the x - y plane. The positive value is indicated by black, and the negative value is indicated by white.

cess. For initial configuration 3, there are three vortex sheets and one current sheet. Namely, there are three current-vortex sheets, and two current sheets are located between the current-vortex sheets. The length of the current sheet is the same as that of the vortex sheet for initial configuration 2, and vice versa. The initial current density and the vorticity are given by j_0 and ω_0 , respectively. Initial j_0 and ω_0 are uniform in the sheet.

The simulation is characterized by three time scales: The Alfvén transit time τ_A , the resistive diffusion time τ_R and the characteristic time scale of the tearing instability $\tau_T = \tau_A^{2/5} \tau_R^{3/5}$. The time scale is normalized by τ_A . The values are $\tau_A = 1$, $\tau_R = 1000$ and $\tau_T = 63.0$. The mesh numbers are 257 in the x direction and 1025 in the y direction. Time step is $\Delta T = 10^{-4}$. The second-order scheme is used for numerical calculations. We adopt free boundary conditions at all the edges of the simulation box, because the sheets do not deform in the x direction near the upper and lower boundaries, if periodic boundary conditions are used, and we consider that the deformation of the sheet is important for the filamentation. The values of the electric current density j_0 and the vorticity ω_0 are chosen as unity.

III. SIMULATION RESULTS

Time evolutions of the distributions of the electric current density j_z , the vorticity ω_z , the magnetic vector potential A_z and the stream function for the velocity field ψ_z on the x - y plane are plotted in Figs. 3–5. The figures show contour plots of them. The stream function is defined by

$$\psi_z(\mathbf{r}) = -\frac{1}{2\pi} \int \omega_z(\mathbf{r}') \ln|\mathbf{r} - \mathbf{r}'| d\mathbf{r}'. \quad (8)$$

The positive value is indicated by black, and the negative value is indicated by white. Initial configurations 1–3 are

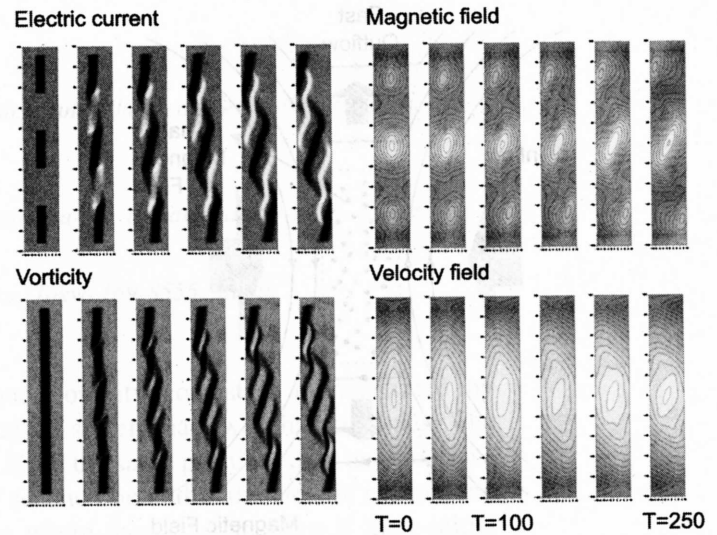


FIG. 4. Time evolutions of the distributions of the electric current density, the vorticity, the magnetic vector potential and the stream function for the velocity field for type (b) are shown. They are plotted in the same manner as Fig. 3.

used for the simulations shown in Figs. 3–5, respectively. From now on, we call the simulation results shown in Figs. 3–5, as types (a)–(c), respectively.

For type (a) shown in Fig. 3, we can see that the vortex sheet slightly rotates counterclockwise. This is because no periodic boundary conditions are used, and the sheet has positive (directed to positive z) vorticity. The current sheet also moves simultaneously, staying overlapped with the vortex sheet. This implies the strong correlation between the electric current and the vorticity. Once they share the same position on the x - y plane, they tend to move simultaneously with each other.

For type (b) shown in Fig. 4, the magnetic reconnection occurs, because the electric current (indicated by white areas) is induced between the magnetic islands. Three magnetic islands are deformed by the flow induced by the vor-

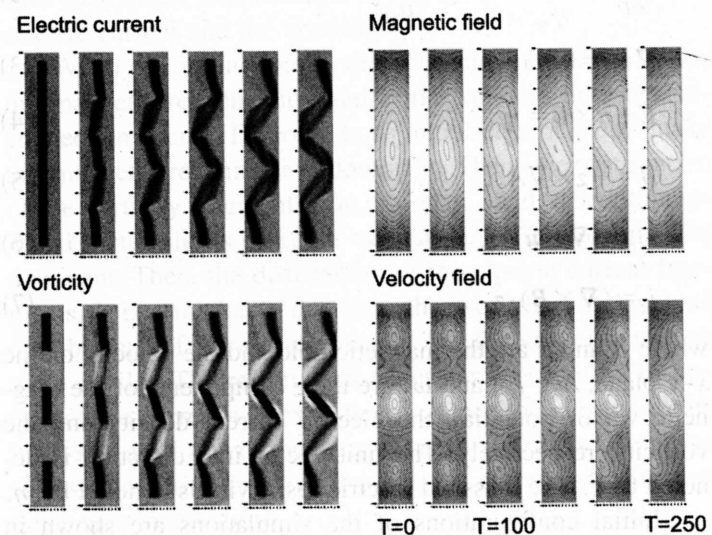


FIG. 5. Time evolutions of the distributions of the electric current density, the vorticity, the magnetic vector potential and the stream function for the velocity field for type (c) are shown. They are plotted in the same manner as Fig. 3.

ticity. On the other hand, the vortex sheet is split into some pieces with time, following the distribution of the electric current. Because the topology of the stream function is not changed so much compared with that of the magnetic field, we consider the velocity field line reconnection is not a main process in this case. It is important that new configurations appear in the distributions of the electric current and the vorticity after $T=100$. They exhibit very similar forms. This means that the electric current and the vorticity occupy the same position on the x - y plane. The structure is rather more filament-like than sheet-like. Once the filaments are formed, they survive stably. This is due to the strong correlation between the electric current and the vorticity, which is shown in Fig. 3.

For type (c) shown in Fig. 5, the velocity field line reconnection occurs, and the topology of the stream function gradually changes with time. The vorticity is induced between the islands of the stream function. In this case, positive vorticity and negative vorticity appear simultaneously. This is related to the conservation of the vorticity in two-dimensional ideal MHD. Because the topology of the magnetic field is not changed so much, compared with that of the stream function, we consider that the magnetic reconnection is not a main process in this case. We can still see the same fragmentation process as in Fig. 4. Namely, the current sheet is split into some pieces with time, following the distribution of the vorticity. The resulting distributions of the electric current and the vorticity show a very similar form in this case also.

Thus we conclude the following points from the results shown in Figs. 4 and 5. The similar distributions for the electric current and the vorticity are formed during the time evolution, even if the initial distributions are not the same. The structure is rather more filament-like than sheet-like, and we consider that the current-vortex filaments are formed. The processes are driven by either the tearing or the Kelvin-Helmholtz instability. Once the filaments are formed, they survive stably. These results give a basis for the MHD model based on the current-vortex filament.

From these simulation results, it is obvious that the positive electric current does not always align with the positive vorticity. There are some cases where the positive electric current aligns with the negative vorticity, as is shown in Figs. 4 and 5. To discuss the alignment quantitatively, we introduce an alignment factor. We define two types of alignment factor. One is a total alignment factor $C_1(t)$ and the other is an antiparallel alignment factor $C_2(t)$. The total alignment factor indicates the ratio of area where the electric current and the vorticity "coexist" to the total area where they "exist." The antiparallel alignment factor indicates the ratio of area where the electric current and the vorticity coexist and align in the antiparallel directions to the total area where they exist. They are defined by

$$C_1(t) = \frac{\int |j_z(t)| \cdot |\omega_z(t)| dS}{\sqrt{\int j_z^2(t) dS} \sqrt{\int \omega_z^2(t) dS}}, \quad (9)$$

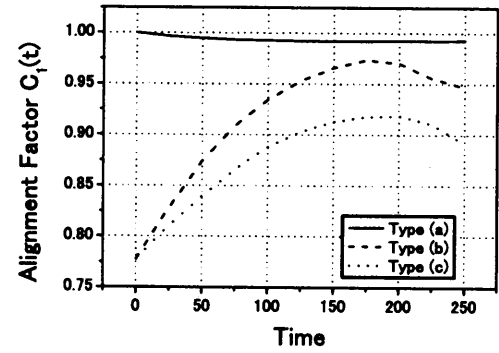


FIG. 6. Time evolutions of the total alignment factor $C_1(t)$ are plotted.

$$C_2(t) = \frac{\int [|j_z(t)| \cdot |\omega_z(t)| - j_z(t) \cdot \omega_z(t)] dS}{\sqrt{\int j_z^2(t) dS} \sqrt{\int \omega_z^2(t) dS}}, \quad (10)$$

where the integrals are performed on the x - y plane in the simulation box.

The maximum and minimum values of $C_1(t)$ are unity and zero, respectively. In the case of $C_1(t)=1.0$, the electric current and the vorticity fully overlap and align in either the parallel or antiparallel direction. In the case of $C_1(t)=0.0$, no electric current overlaps with the vorticity, although there are electric current and vorticity on the x - y plane. The maximum and minimum values of $C_2(t)$ are unity and zero, respectively. In the case of $C_2(t)=1.0$, the electric current and the vorticity fully overlap and align in the antiparallel direction. In the case of $C_2(t)=0.0$, there are two possibilities. One is that no electric current overlaps with the vorticity. The other is that all the electric current and the vorticity align in the parallel direction.

Time evolutions of the alignment factors $C_1(t)$ and $C_2(t)$ for types (a)–(c) are shown in Figs. 6 and 7, respectively. For type (a), the total and antiparallel alignment factors become approximately constant after $T=50$, and the values are $C_1(t)=0.99$ and $C_2(t)=0.00$. This indicates that the electric current and the vorticity, whose initial directions are positive z , do not change their directions during the evolution and stay overlapped with each other. This result gives evidence of the strong correlation between the electric current and the vorticity.

For types (b) and (c), similar evolutions of the alignment factors are observed. The initial values of $C_1(t)$ are not equal

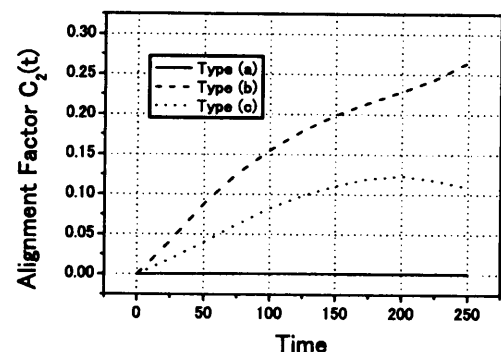


FIG. 7. Time evolutions of the antiparallel alignment factor $C_2(t)$ are plotted.

to unity for these cases. This is because there are areas where either the electric current or vorticity only exists initially. We have seen that the distributions of the electric current and the vorticity become similar during the evolution in Figs. 4 and 5. In fact, the evolutions of the $C_1(t)$ tell us that they evolve to create more overlapping regions through the evolution. When they align, the directions of the electric current and the vorticity are, however, not uniform, because the values of $C_2(t)$ for types (b) and (c) increase with time, while they are uniform for type (a). The value of $C_2(t)$ for type (b) is larger than that for type (c). This is because the directions of the induced current by the magnetic reconnection are almost positive z , while the directions of the induced vorticity are half positive and half negative. The most important point is that the values of $C_1(t)$ and $C_2(t)$ gradually increase with time for types (b) and (c), even if the initial distributions of the electric current and the vorticity are not the same. Thus, we conclude that the alignment occurs for these cases. It is a good reason to consider that the electric current and the vorticity form the current-vortex filaments.

IV. CONCLUSIONS

We demonstrated the time evolution of the current-vortex sheet via the numerical simulations.

When initial spatial distributions of the electric current and the vorticity are the same, the electric current and the vorticity tend to move simultaneously, staying overlapped with each other. This means a strong correlation between the electric current and the vorticity.

When initial spatial distributions are not the same, the magnetic reconnection and/or the velocity field line recon-

nection occurs. When the magnetic reconnection is dominant, the distribution of the vorticity fragments. On the other hand, when the velocity field line reconnection is dominant, the distribution of the electric current fragments. It is remarkable that in both cases, the time-evolved distributions of the electric current and the vorticity become quite similar forms, even if their initial spatial distributions are not the same. The resulting distributions indicate the formation of the current-vortex filaments. Once the current-vortex filaments are formed, they survive stably. This is due to the strong correlation between the electric current and the vorticity.

Now we are carrying out research work on the MHD simulation based on the current-vortex filaments in detail and will report this elsewhere.

ACKNOWLEDGMENT

This work is supported by Special Postdoctoral Research Program at RIKEN.

¹D. Biskamp, E. Schwarz, Z. Zeiler, A. Celani, and J. F. Drake, *Phys. Plasmas* **6**, 751 (1999).

²E. R. Priest, *Phys. Plasmas* **4**, 1945 (1997).

³G. E. Vekstein and R. Jain, *Phys. Plasmas* **5**, 1506 (1998).

⁴M. Ugai, *Phys. Plasmas* **6**, 1522 (1999).

⁵Y. Yatsuyanagi, T. Hatori, and T. Kato, *Earth, Planets, Space* **53**, 615 (2001).

⁶Y. Yatsuyanagi, T. Hatori, and T. Kato, *J. Plasma Phys.* **62**, 493 (1999).

⁷Y. Yatsuyanagi, T. Hatori, and T. Kato, *J. Phys. Soc. Jpn.* **65**, 745 (1996).

⁸Y. Yatsuyanagi, T. Hatori, and T. Kato, *J. Phys. Soc. Jpn.* **67**, 166 (1998).

⁹R. B. Dahlburg, P. Boncinelli, and G. Einaudi, *Phys. Plasmas* **4**, 1213 (1997).